Electrical transport properties of $YCo_{1-x}Mn_xO_3$ ($0 \leq x \leq 0.2$) prepared by sol–gel process*

Liu Yi(刘 义)[a)b)†] and Li Hai-Jin(李海金)[a)b)]

[a)] School of Mathematics and Physics, Anhui University of Technology, Ma'anshan 243032, China
[b)] Institute of Optoelectronic Information Materials and Technologies, Anhui University of Technology, Ma'anshan 243032, China

(Received 21 September 2014; revised manuscript received 7 November 2014; published online 10 February 2015)

Mn substitution compounds $YCo_{1-x}Mn_xO_3$ ($0 \leq x \leq 0.2$) are synthesized by using the sol–gel process. Electrical transport properties of $YCo_{1-x}Mn_xO_3$ are investigated in the temperature range from 200 K to 780 K. The experimental results show that after Mn substitution the electrical resistivity of $YCo_{1-x}Mn_xO_3$ first increases, then decreases, which is due to the electrons introduced by Mn doping. The sign of Seebeck coefficient for $YCo_{1-x}Mn_xO_3$ ($x \neq 0$) is positive or negative, which is also proved by the Hall coefficient measurement. Moreover, at about room temperature, the Seebeck coefficient of $YCo_{1-x}Mn_xO_3$ with 1% doping Mn content becomes a negative value, whose absolute value is maximum; furthermore, the absolute value gradually decreases with increasing the Mn substitution content, which can be explained by the double carrier model.

Keywords: perovskite cobalt oxides, sol–gel process, electrical transport

PACS: 72.20.Pa, 72.80.Ga, 61.05.cp **DOI:** 10.1088/1674-1056/24/4/047202

1. Introduction

In recent years, much attention has been paid to rare-earth cobalt oxide $RCoO_3$ (R represents the rare-earth element) because of its interesting electrical and magnetic properties.[1–3] $RCoO_3$ oxide has a large thermopower, which is one of the important requirements for a thermoelectric material with good performance,[4] therefore, it is also investigated as a good candidate for thermoelectric applications. In 2004, Androulakis et al. found that the figure of merit ZT value for $La_{0.95}Sr_{0.05}CoO_3$ was 0.18,[5] which stimulated the interest in investigating oxide thermoelectric materials.

$YCoO_3$ has a distorted perovskite structure[6,7] with orthorhombic symmetry (space group $Pbnm$ ($Z = 4$)) and six oxygen atoms surround each cobalt ion. $YCoO_3$ has a large thermopower $S \sim 1039$ $\mu V \cdot K^{-1}$ [4] and small thermal conductivity $\kappa \sim 5.39$ $W \cdot m^{-1} \cdot K^{-1}$ [4] at about room temperature, the large thermopower and small thermal conductivity are two preconditions for having good thermoelectric performance, therefore, scientists have also considered $YCoO_3$ as a thermoelectric material candidate. Our group systematically investigated thermoelectric properties and physical mechanisms of $YCoO_3$ based thermoelectric materials by doping or substitution.[4,8–12] We successfully substituted Ca for Y in $YCoO_3$ to reduce its electrical resistivity, and we estimated its thermoelectric performance. Moreover, the experimental results show that the temperature dependence of electrical resistivity for $Y_{1-x}Ca_xCoO_3$ is consistent with the small-polaron hopping conduction model. For the Sr-substituted sample $Y_{1-x}Sr_xCoO_3$, Sr substitution results in reducing its electrical resistivity, and effectively improving its thermoelectric properties. The substitution of Ni for the Co site in $YCo_{1-x}Ni_xO_3$ indicates that its electrical resistivity decreases and the high-temperature thermoelectric properties are improved. However, the conduction mechanism of $YCoO_3$ has hardly been investigated. In order to understand in the round the conduction mechanisms of $YCoO_3$ based materials, we will substitute Mn into Co site in $YCoO_3$, and investigate the conduction mechanisms and behaviors of $YCoO_3$ based material.

2. Experimental details

Manganese doped oxides $YCo_{1-x}Mn_xO_3$ were prepared stoichiometrically from $Y(NO_3)_3 \cdot 6H_2O$ (99.5%), $Co(NO_3)_2 \cdot 6H_2O$ (99.0%), and $Mn(NO_3)_2$ (50%) solution. $0.02x$ ($x = 0$, 0.01, 0.05, 0.15, 0.20) mol of $Mn(NO_3)_2$, 0.02 $(1-x)$ mol of $Co(NO_3)_2 \cdot 6H_2O$ (99.0%), and 0.02 mol of $Y(NO_3)_3 \cdot 6H_2O$ (99.0%) were dissolved in 20 ml of an aqueous solution of 0.02 mol citric acid (99.5%) by using deionized water. The solutions were continuously stirred for about 1 h, resulting in a homogenization of Mn^{2+}, Co^{2+} and Y^{3+} cations in the mixture solution. Subsequently, the mixtures were slowly heated to 90 °C, and at this temperature they were dried for 12 h, forming a brown powder from the mixtures. The brown powders were calcined in air at atmospheric pressure in a muffle furnace at 300 °C for 2 h, forming black powder samples, so as to remove organic compounds. Then, these powder samples were ground and subsequently compressed into pellets 13 mm in diameter. Finally, bulk samples were obtained by sintering the green pellets in air in a

*Project supported by the Anhui Provincial Science Key Foundation of Higher Education Institutions, China (Grant No. KJ2011A053) and the National Natural Science Foundation of China (Grant No. 51202005).

†Corresponding author. E-mail: yliu6@ahut.edu.cn

© 2015 Chinese Physical Society and IOP Publishing Ltd

tube furnace at 900 °C for 120 h, subsequently followed by spontaneously cooling slowly down to room temperature in the furnace.

Phase structures and the lattice constant for the obtained compounds were determined by using x-ray diffraction (XRD) (Philips-X PERT PRO diffractometer) with Cu K_α irradiation at room temperature. The accurate lattice parameters were determined from the d-value of the XRD peaks using a standard least-squares refinement method with an Si standard for calibration. To measure their electrical resistivity, bar-shaped specimens of the size $(\sim)12$ mm $\times(\sim)2$ mm $\times(\sim)1.0$ mm were cut from the bulk samples. The electrical resistivity and Seebeck coefficient were measured on a computer-assisted device. DC electrical resistivities were measured in a vacuum by a conventional standard four-probe method in the temperature range from 200 K to 720 K. The Seebeck coefficient was also measured in a vacuum in the temperature range from 300 K to 780 K. The carrier concentration was determined by measuring the Hall coefficient at room temperature in a magnetic field $H = 0.73$ T.

3. Results and discussion

3.1. Phase determination and change of lattice parameters for $YCo_{1-x}Mn_xO_3$

Figure 1 shows the room-temperature XRD patterns of $YCo_{1-x}Mn_xO_3$ ($x = 0$, 0.01, 0.03, 0.05, 0.10, 0.20). One can see that the main diffraction peaks of $YCoO_3$ are in accordance with the indexed standard JCPDS card (No. 88-0425), and the main diffraction peaks of doped samples $YCo_{1-x}Mn_xO_3$ ($x \neq 0$) are also in agreement with the standard JCPDS card. Moreover, the XRD diffraction peaks of $YCoO_3$ are the same as those of the compounds synthetized by Liu *et al.*[8] and Thornton *et al.*[3] In addition, the calculated lattice parameters (a, b, and c) with a permissible error range $\pm 0.05\%$ increase with the increase of Mn concentration, which are plotted in corresponding panels, and the volume unit cell versus Mn concentration is shown in the remaining panel in Fig. 2. Therefore, these indicate that Mn has been substituted for Co of $YCoO_3$, and the substituted compounds $YCo_{1-x}Mn_xO_3$ have formed.

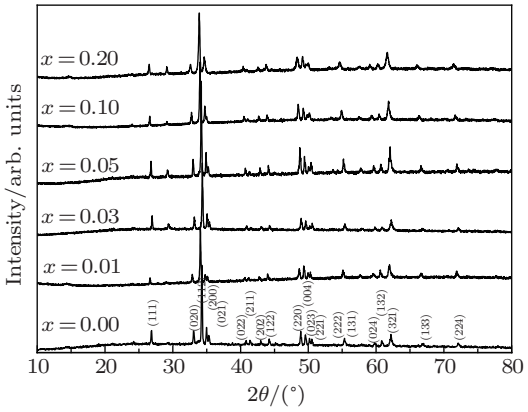


Fig. 1. XRD patterns (Cu K_α irradiation) for $YCo_{1-x}Mn_xO_3$.

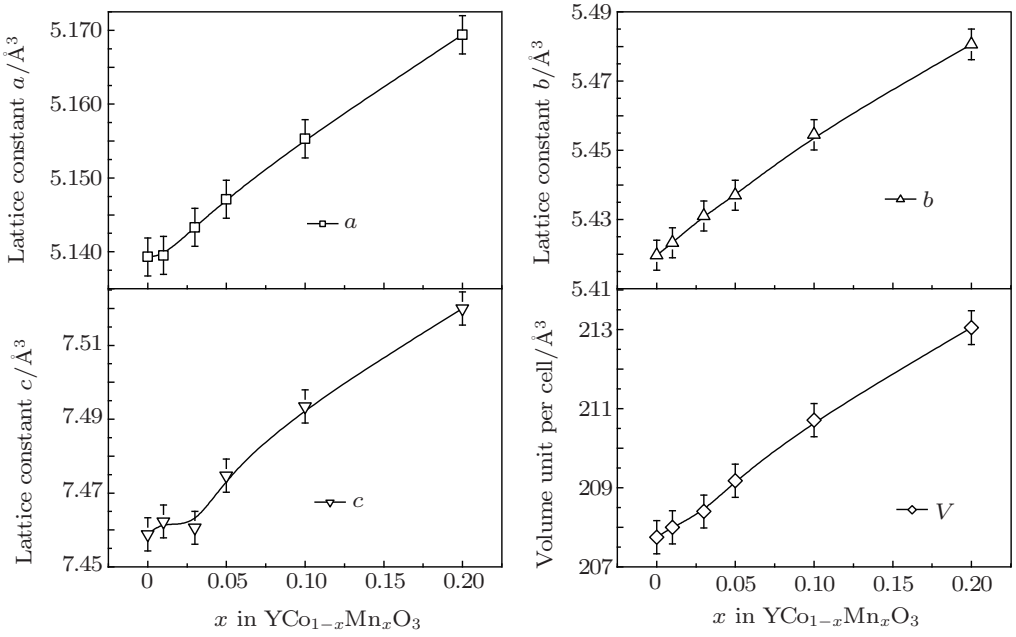


Fig. 2. Lattice constants a, b, c, and volume per unit cell V for $YCo_{1-x}Mn_xO_3$.

3.2. Resistivities and its temperature dependences for $YCo_{1-x}Mn_xO_3$

The temperature dependences of electrical resistivity for $YCo_{1-x}Mn_xO_3$ samples are shown in Fig. 3. To clearly show the electrical resistivity of $YCo_{1-x}Mn_xO_3$ in the whole temperature range, the longitudinal axis (electrical resistivity) is plotted on a logarithm scale. One can see that the electrical resistivity of the $YCoO_3$ sample has a gradual decrease

with the increase of temperature in the whole temperature range. After Mn substitution, great changes take place in the temperature dependences of electrical resistivity for samples $YCo_{1-x}Mn_xO_3$ ($x \neq 0$), that is, as temperature rises, the electrical resistivity of $YCo_{1-x}Mn_xO_3$ decreases almost exponentially. For instance, the electrical resistivity of the $x = 0.05$ sample decreases from $\sim 6.65 \times 10^3$ Ω·m at 160 K to ~ 0.88 Ω·m at 450 K, then to ~ 0.014 Ω·m at 670 K. Moreover, after Mn doping in $YCoO_3$, the electrical resistivities of samples $YCo_{1-x}Mn_xO_3$ ($x \neq 0$) increase at low temperature $T < 500$ K, for example, the room-temperature electrical resistivity increases from 6.9 Ω·m for sample $x = 0$ to 1.58×10^2 Ω·m for $x = 0.01$, 57.7 Ω·m for $x = 0.03$, 39.9 Ω·m for $x = 0.05$, 35.0 Ω·m for $x = 0.1$, and 82.3 Ω·m for $x = 0.2$, which is due to the change of carrier concentration as indicated in Table 1. For a small amount of substituted Mn element content ($x = 0.01$), the electrical resistivity has a great change. This is due to the electrons induced mainly by Mn substitution, for $YCoO_3$ is hole conduction,[4] which results in a decrease in hole concentration. The carrier mobility also shows the same result, that is, it decreases from 0.61 $cm^2 \cdot V^{-1} \cdot S^{-1}$ down to 0.18 $cm^2 \cdot V^{-1} \cdot S^{-1}$ (Table 1).

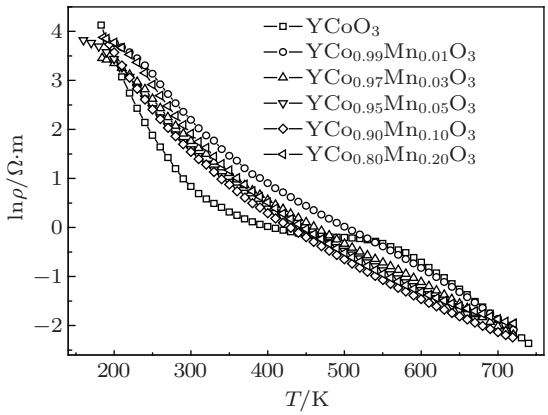


Fig. 3. Temperature dependence of electrical resistivity ρ of $YCo_{1-x}Mn_xO_3$.

Table 1. Values of room-temperature resistivity ρ_{rt}, carrier concentration n_p (n_e), and carrier mobility μ_p (or μ_e) for $YCo_{1-x}Mn_xO_3$.

x	0	0.01	0.03	0.05	0.10	0.20
ρ_{rt}/Ω·m	6.92	1.58×10^2	57.7	39.9	35.0	82.3
n_p (or n_e)/10^{15} cm^{-3}	6.1×10^{-1}	-1.80×10^{-1}	–3.77	–1.90	-2.46×10^{-1}	–1.31
μ_p (or μ_e)/$cm^2 \cdot V^{-1} \cdot S^{-1}$	10.4	1.01	0.14	0.41	0.35	0.25

However, at high temperature $T > 500$ K, the electrical resistivity of the doping sample is smaller than that of the $YCoO_3$ sample, and the electrical resistivity of each of the samples almost tends to a constant value at the highest temperature. The reason is that the conductivity of $YCo_{1-x}Mn_xO_3$ is related to the electrical configuration of Co ions,[4] the doping Mn element affects the change of the spin state of Co ions, resulting in the change in electrical resistivity.

From Fig. 2, one can see that the Mn doping for the $YCoO_3$ sample gives rise to the enlargement in the volume unit per cell, indicating that when a Mn element substitutes for Co, the Mn ion is mainly in the form of a Mn^{3+} ion, because the Mn^{3+} ion radius (0.66 Å) is larger than the Co^{3+} (0.63 Å) ion radius. However, this does not exclude the existence of Mn^{4+} ionic in $YCo_{1-x}Mn_xO_3$. The partial Mn^{4+} ions act as donors offering electrons. These electrons will compensate for those holes in the acceptor impurity (or defect) level, bringing on a great decrease of hole concentration, thus resulting in a significant increase in electrical resistivity. However, with the increase in dopping Mn content, more Mn^{4+} ions will be introduced, in addition to the electrons as the donor to compensate for those holes in the acceptor impurity (or defect) level, other electrons will be ionized into the conduction band, causing the obvious electron conduction. When the double carriers (electron and hole) conduct electricity, the total resistivity can be expressed as,[13]

$$\rho = \frac{1}{q\left(n_e\mu_e + n_p\mu_p\right)},$$

where q is the electrical charge of the carrier, n_e is the electron concentration, n_p is the hole concentration, μ_e is the electron mobility, and μ_p is the hole mobility. One can see from the equation of the double carrier conduct that as the Mn content increases, the electron concentration of $YCo_{1-x}Mn_xO_3$ ($x > 0.1$) increases, then it results in a decrease of electrical resistivity.

For comprehending in more detail the temperature of electrical resistivity for $YCo_{1-x}Mn_xO_3$, plots of the logarithm of electrical resistivity ρ versus the reciprocal of temperature T are shown in Fig. 4. We can note that there are two good linear relations between $\ln\rho$ and $1/T$ at a low temperature range (LTR) ($T < 304$ K for $x = 0$, $T < 450$ K for $x = 0.01$, $T < 405$ K for $x = 0.03$, 0.05, 0.10, 0.20) and high temperature range (HTR) ($T > \sim 455$ K). This indicates that they obey the thermal activation conduction model $\rho = \rho_0 \exp(E_a/\kappa_B T)$ (ρ_0 is a constant, E_a is the activation energy for conduction, κ_B is the Boltzmann constant, and T is the absolute temperature) as shown in Fig. 4. According to the equation $\rho = \rho_0 \exp(E_a/\kappa_B T)$, we obtain the activation energy E_{a1} at LTR and E_{a2} at HTR (Fig. 5). One can see that as the Mn content increases, the activation energy gradually decreases, for instance, at HTR, the activation energy values decrease from

1.024 eV for $x = 0$ to 0.612 eV for $x = 0.05$, then to 0.443 eV for $x = 0.20$, indicating that the carrier conduction becomes stronger with the increase of Mn content. However, the activation energy at LTR is smaller than at HTR, which suggests that the carrier conduction at LTR is much easier than at HTR.

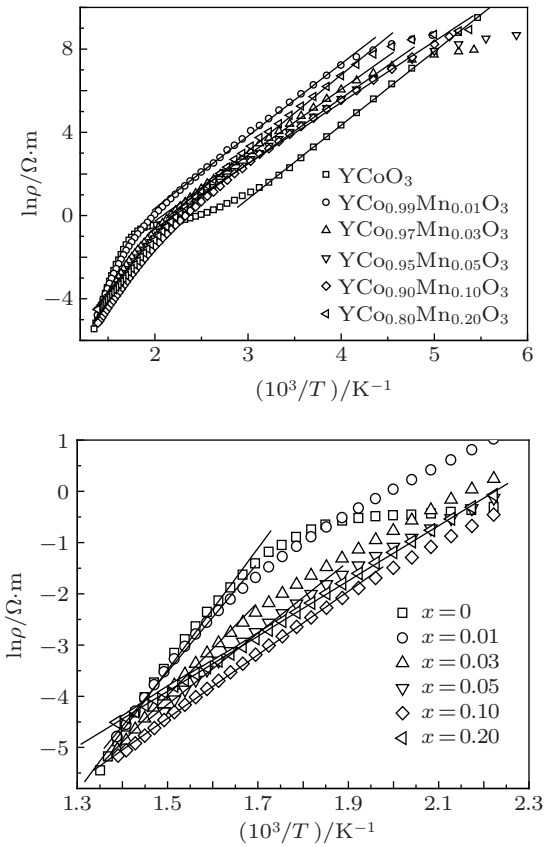


Fig. 4. Logarithmic electrical resistivity ρ versus reciprocal temperature of $YCo_{1-x}Mn_xO_3$.

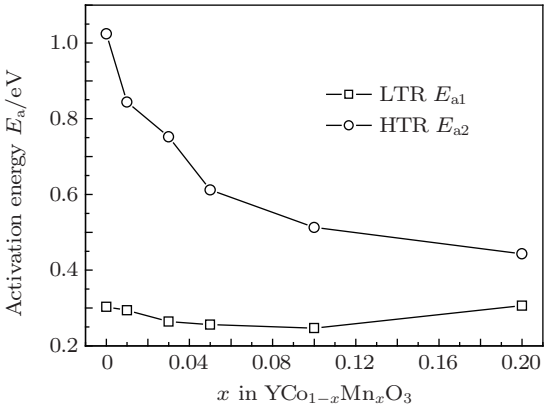


Fig. 5. Activation energy E_a versus x in $YCo_{1-x}Mn_xO_3$.

3.3. Thermopower of $YCo_{1-x}Mn_xO_3$

Figure 6 shows the temperature dependences of Seebeck coefficient S for samples $YCo_{1-x}Mn_xO_3$ ($x = 0$, 0.01, 0.03, 0.05, 0.1, 0.2). The sign of the Seebeck coefficient for $YCoO_3$ is positive over the entire temperature range (300 K–780 K), i.e., p-type conduction, which accords with the result of the Hall coefficient in Fig. 7. However, the sign of Seebeck coefficient for $YCo_{1-x}Mn_xO_3$ ($x \neq 0$) is complicated, for each sample, both positive and negative. At room temperature, with a 1%-doping Mn content, the absolute value of the Seebeck coefficient for $YCo_{0.99}Mn_{0.01}O_3$ becomes the largest value, which is negative, moreover, the absolute value of the Seebeck coefficient for $YCo_{1-x}Mn_xO_3$ gradually decreases with increasing the Mn substitution content, such as, from 574 $\mu V \cdot K^{-1}$ for $x = 0.01$, to 283 $\mu V \cdot K^{-1}$ for $x = 0.05$, to 164 $\mu V \cdot K^{-1}$ for $x = 0.1$, and to 32 $\mu V \cdot K^{-1}$ for $x = 0.2$, which are shown in Fig. 6. In order to get a better understanding of the phenomenon, we measure the room-temperature Hall coefficient R_H for $YCo_{1-x}Mn_xO_3$ as shown in Fig. 7. We can note that the Hall coefficient changes from the positive value (for $x = 0.01$, 0.03 samples) to the negative value (for $x = 0.1$, 0.2 samples), correspondingly; moreover, the Seebeck coefficient changes from the positive value for the $x = 0$ sample to negative value (for $x = 0.01$, 0.03 samples), then gradually increases, which finally tends to a positive value.

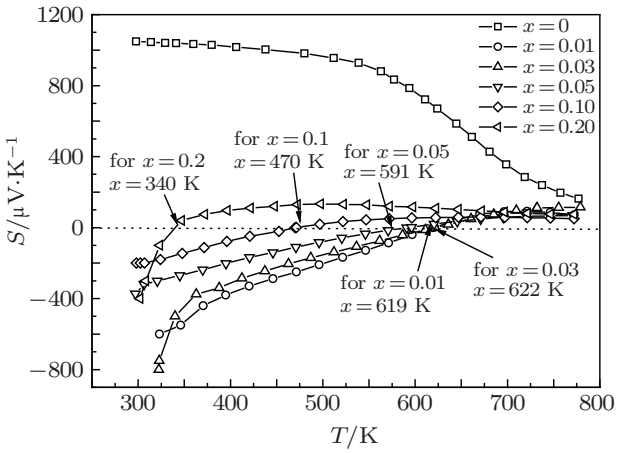


Fig. 6. Temperature dependences of Seebeck coefficient S for $YCo_{1-x}Mn_xO_3$.

The changes of Seebeck coefficient and Hall coefficient R_H can be comprehended by the double carrier model. As the double carriers conduct, the Hall coefficient can be expressed as,[14]

$$R_H = \frac{-n_e\gamma_e\mu_e^2 + n_p\gamma_p\mu_p^2}{q\left(n_e\mu_e + n_p\mu_p\right)^2},$$

where γ_e and γ_p are the Hall factors of electron and hole, respectively. The Hall coefficient of $YCoO_3$ is positive, i.e., $R_H = \gamma_p/n_p q > 0$, $n_p \gg n_e$. With the increase of dopping Mn content, Mn^{4+} ion is introduced, resulting in an increase of electron concentration for $YCoO_3$. These doped electrons will partially offset the hole contribution to the Hall coefficient. Therefore, with increasing the Mn content, the Hall coefficient decreases. From Fig. 7, we can see that as the dopping Mn content arrives at about 5%, $R_H = (3.42 \pm 0.27) \times 10^{-6}$ m^3/C value, compared to $R_H = 2.6$ m^3/C value for the sample $x = 0.01$, tends to 0, that is, $n_e\gamma_e\mu_e^2 = n_p\gamma_p\mu_p^2$.

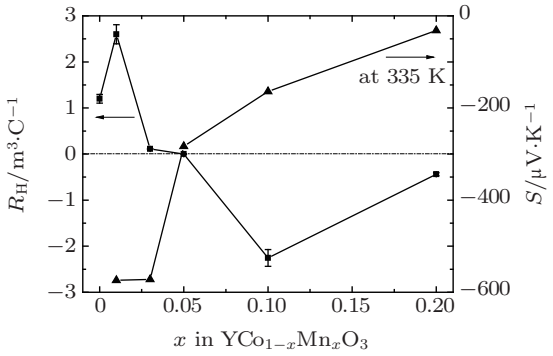


Fig. 7. Hall coefficient R_H and Seebeck coefficient at 335 K versus x in $YCo_{1-x}Mn_xO_3$.

When the double carrier conducts, the Seebeck coeffient can be expressed as,[15]

$$S = \frac{\sigma_n S_n}{\sigma_n + \sigma_p} + \frac{\sigma_p S_p}{\sigma_n + \sigma_p},$$

where $\sigma_n = qn_e\mu_e$ is the electron conductivity, $\sigma_p = qn_p\mu_p$ is the hole conductivity, S_n and S_p are the thermopowers of electron and hole, respectively. Substituting $\sigma_n = qn_e\mu_e$ and $\sigma_p = qn_p\mu_p$ into the above equation, we can obtain

$$S = \frac{n_e\mu_e S_n + n_p\mu_p S_p}{n_e\mu_e + n_p\mu_p}.$$

We can see from the above equation that the Seebeck coefficient is determined in n_e (or n_p), μ_e (or μ_p), S_n, and S_p. As the Mn doping content is $x = 0.01$, a few electrons are introduced. At present, electrons exist in a nondegenerate state, thereby making the Seebeck coefficient larger because of $S \propto 1/n$, resulting in $n_e\mu_e S_n > n_p\mu_p S_p$. Therefore, the Seebeck coefficient for the sample with $x = 0.01$ becomes a positive value. With the increase of the doped Mn content, n_e increases, the absolute value of S_n decreases, and the total absolute value of $n_e\mu_e S_n$ decreases; therefore, the total absolute value of S decreases.

In addition, one can see that the Seebeck coefficients of $YCo_{1-x}Mn_xO_3$ at high temperature ($T \sim 800$ K) all tends to a limit value, because the Seebeck coefficient of $YCo_{1-x}Mn_xO_3$ at high temperature is associated with the electrical configuration of Co ions.[4]

4. Conclusions

Electrical transport properties of Mn substitution compounds $YCo_{1-x}Mn_xO_3$ ($0 \le x \le 0.2$), prepared by using the sol–gel process, are investigated in the temperature range from 200 K to 780 K. The results show that after Mn substitution, the electrical resistivity of $YCo_{1-x}Mn_xO_3$ first increases, then decreases at temperature $T < 500$ K, which is due to the electrons introduced by Mn doping; at the highest temperature, the electrical resistivity of $YCo_{1-x}Mn_xO_3$ approaches to a value relating to the electrical configuration of Co ions. The sign of Seebeck coefficient for $YCo_{1-x}Mn_xO_3$ ($x \neq 0$) is positive or negative for each sample, which is also proved by Hall coefficient measurement. Moreover, at about room temperature and with doping Mn content being 1%, the Seebeck coefficient becomes negative and its aboslute value is maximum, furthermore, the Seebeck coefficient absolute value of $YCo_{1-x}Mn_xO_3$ gradually decreases with increasing the Mn substitution content, which is explained by the double carrier model.

References

[1] Raccah P M and Goodenough J B 1967 *Phys. Rev.* **155** 932
[2] Bhide V H, Rajoria D S, Rao G Ramma and Rao C N R 1972 *Phys. Rev. B* **6** 1021
[3] Thornton G, Morrison F C, Partington S, Tofield B C and Williams D E 1988 *J. Phys. C: Solid State Phys.* **21** 287
[4] Liu Y, Qin XY, Wang Y F, Xin H X, Zhang J and Li H J 2007 *J. Appl. Phys.* **101** 083709
[5] Androulakis J, Migiakis Pantelis and Giapintzakis J 2004 *Appl. Phys. Lett.* **84** 1099
[6] Mehta Apurva, Berliner R and Smith Robert W 1997 *J. Solid State Chem.* **130** 192
[7] Knížek K, Jirák Z, Hejtmánek J, Veverka M, Maryško M, Hauback B C and Fjellvåg H 2006 *Phys. Rev. B* **73** 214443
[8] Liu Y and Qin X Y 2006 *J. Phys. Chem. Solids* **67** 1893
[9] Liu Y, Li H J, Zhang Q and Liu H T 2012 *Chin. J. Mater. Res.* **26** 31
[10] Liu Y, Zhang Q, Li H J and Liu H T 2013 *Acta Phys. Sin.* **62** 047202 (in Chinese)
[11] Liu Y, Li H J and Li Y 2013 *Ceram. Inter.* **39** 8189
[12] Liu Y, Li H J, Zhang Q, Li Y and Liu H T 2013 *Chin. Phys. B* **22** 057201
[13] Chen H S 1987 *The Handbook about Physical Properties of Metal Materials*, Vol. 1: *Physical Properties and Test Method of Metal* (Beijing: Metallurgical Industry Press)
[14] Feng D and Jin G J 2003 *Introduction to Condensed Matter Physics*, Vol. 1 (Beijing: Higher Education Press)
[15] MacDonald D K C 1962 *Thermoelectricity: an Introduction to the Principles* (London: John Wiley & Sons Press)